Title
Non-directed allylic C–H acetoxylation in the presence of Lewis basic heterocycles

Journal
Chemical Science, 5(6)

ISSN
2041-6520

Authors
Malik, Hasnain A
Taylor, Buck LH
Kerrigan, John R
et al.

Publication Date
2014

DOI
10.1039/c3sc53414f

Peer reviewed

Published in final edited form as:
Chem Sci. 2014 June 1; 5(6): 2352–2361. doi:10.1039/C3SC53414F.

Non-Directed Allylic C–H Acetoxylation in the Presence of Lewis Basic Heterocycles

Hasnain A. Malik[a], **Buck L. H. Taylor**[b], **John R. Kerrigan**[a], **Jonathan E. Grob**[a], **K. N. Houk**[b], **J. Du Bois**[c], **Lawrence G. Hamann**[a], and **Andrew W. Patterson**[a]

[a]Global Discovery Chemistry, Novartis Institutes for BioMedical Research, Inc., Cambridge, Massachusetts 02139

[b]Department of Chemistry and Biochemistry, University of California, Los Angeles, California 90095

[c]Department of Chemistry, Stanford University, Stanford, California 94305

Abstract

We outline a strategy to enable non-directed Pd(II)-catalyzed C–H functionalization in the presence of Lewis basic heterocycles. In a high-throughput screen of two Pd-catalyzed C–H acetoxylation reactions, addition of a variety of *N*-containing heterocycles is found to cause low product conversion. A pyridine-containing test substrate is selected as representative of heterocyclic scaffolds that are hypothesized to cause catalyst arrest. We pursue two approaches in parallel that allow product conversion in this representative system: Lewis acids are found to be effective *in situ* blocking groups for the Lewis basic site, and a pre-formed pyridine *N*-oxide is shown to enable high yield of allylic C–H acetoxylation. Computational studies with density functional theory (M06) of binding affinities of selected heterocycles to $Pd(OAc)_2$ provide an inverse correlation of the computed heterocycle–$Pd(OAc)_2$ binding affinities with the experimental conversions to products. Additionally, ^{1}H NMR binding studies provide experimental support for theoretical calculations.

Introduction

The ability to selectively convert abundant and otherwise inert C–H bonds to C–X substituent groups has widespread potential for applications in the synthesis of pharmaceuticals, natural products, agrochemicals, polymers, and feedstock commodity chemicals.[1–13] Among emerging methods, Pd(II)-catalyzed allylic C–H functionalization reactions are a particularly versatile means to generate chemical diversity,[14–23] exploiting the ubiquitous olefin functionality that is readily installed and differentiated using a wide array of chemical reactions.[24] Despite these technological advances, a major unmet challenge associated with C–H functionalization methods is the lack of reactivity and/or chemoselectivity in systems where Lewis basic moieties are present. The lack of Lewis

Electronic Supplementary Information (ESI) available: [details of any supplementary information available should be included here]. See DOI: 10.1039/b000000x/

basic functional group compatibility in Pd-catalyzed allylic C–H functionalization severely limits the generality and applicability of these transition metal-catalyzed methodologies in pharmaceutical research, where heterocyclic moieties are routinely encountered.[25–28] In order to address this problem, we have explored allylic C–H oxidation in the context of heterocycle-containing compounds typical of pharmaceutical agents. While Lewis basic functionalities have been employed for directed C–H activation,[8,11] they generally impede alternate non-directed C–H functionalization reactivity (Figure 1).[27–35] These issues have been addressed in the context of transition metal-catalyzed olefin metathesis,[36] but they have yet to be investigated within the framework of C–H activation. Herein, we describe two strategies to block the Lewis basic sites that would otherwise have a deleterious effect on the desired C–H activation process. These findings should expand the scope of Pd-catalyzed allylic C–H oxidation and provide a high-throughput method of analysis for determining functional group compatibility in other transition metal-mediated reaction processes.

Results

High-throughput heterocycle screen for chemical robustness

We wished to establish a rigorous and high-throughput method to evaluate functional group compatibility in non-directed allylic C–H bond functionalization reactions. Initial experiments were performed to determine levels of conversion for representative allylic C–H acetoxylation reactions on a control substrate **1** using methods disclosed by the groups of White and Stahl (reactions A and B, respectively, Figure 2).[18,23] Interestingly, catalyst choice enables access to either allylic acetate regioisomer **2** or **3** with high levels of regiocontrol with the $Pd(OAc)_2$/$PhS(O)C_2H_4S(O)Ph$/*p*-benzoquinone-combination favoring the branched product and the $Pd(OAc)_2$/4,5-diazafluorenone-catalyst favoring the linear product. As postulated in Figure 3, the divergence of this observed regioselectivity resulting from ligand selection is likely a consequence of mechanistically distinct reductive elimination pathways. In reaction A, the sulfoxide ligand is proposed to be initially displaced by acetate, and subsequently the Pd-catalyst is coordinated with *p*-benzoquinone. From this complex the terminus of the olefin is sterically blocked by the benzoquinone ligand, thus causing inner-sphere attack of the acetate to form the branched product.[18] However, the possibility of a non-obvious participation of the bissulfoxide ligand in the reductive elimination step cannot be entirely excluded. In reaction B, the bis-ligated 4,5-diazafluorenone may occupy a coordinatively saturated Pd-complex, favoring outer-sphere attack of the acetate to form the preferred linear product.[23] Alternatively, a mono-*N*-ligated Pd-complex may give rise to an inner-sphere reductive elimination mechanism to form the linear product. There are ongoing efforts to study these mechanistic possibilities, the results of which will be reported in due course.

We then attempted the same transformations in the presence of a variety of heterocyclic fragment additives in an array format in a high-throughput robustness screen (Figure 4). While in the process of conducting this research, Collins and Glorius disclosed an elegant and similar account utilizing such a high-throughput robustness screen in a quantitative fashion for the Buchwald-Hartwig C–N cross-coupling reaction,[28,39a] among others.[39b–e]

Such screens allow for the rapid evaluation of functional group compatibility as well as the generality of the selected reaction conditions. Buchwald and coworkers recently disclosed a related account describing coordination-mediated catalyst arrest in the Suzuki-Miyaura cross-coupling reaction.[40] For our purposes, both starting material and products are readily identifiable via LC-MS analysis, enabling an accurate estimation of product conversion. We observed that the heterocycle fragments that we expected to strongly coordinate to the Pd(II)-catalyst resulted in deleterious reaction outcome, specifically low conversion to product under both sets of reaction conditions. Generally, a higher level of product formation was observed using the $Pd(OAc)_2$/4,5-diazafluorenone-catalyst system (reaction B).

It was observed that heterocycles **4–10** had the least degree of adverse impact on reaction outcome. Empirically, these heterocycle fragments may be the least strongly coordinating (to Pd-catalyst) of the set, thereby being the most compatible with desired product formation. Holding true to prediction, the inclusion of highly coordinating fragments **11–14** and **16–22** impeded reactivity in both reaction systems A and B. While fragment **15** did not greatly effect reaction outcome in reaction B, it was detrimental in reaction A.

Validating the high-throughput screen's predictive potential

Corroborating the predictive potential of the high-throughput screen, in our case identifying the heterocyclic motifs that are or are not amenable to enabling a particular chemical transformation, is of considerable significance to discovery and process chemists as well as the synthetic community as a whole.[28] Discerning the applicability of a particular chemical transformation towards both target-oriented synthesis and diversification endeavors prior to synthetic efforts would be valuable. Thus, having completed our high-throughput heterocycle screen, we were keen to validate our findings with substrates incorporating representative heterocyclic fragments. We selected a distribution of heterocycles (**5**, **8**, **11**, **13**, and **17**) that fall within all of the general categories defined by the levels of conversion using the two allylic C–H functionalization methods screened.

In the high-throughput screen (Figure 4), the carbazole fragment **5** had little negative influence on product conversion in either set of reaction conditions. When a carbazole-containing olefin substrate **23** was subjected to either reaction A or B, 67% (80:20 *b:l*) and 72% (16:84 *b:l*) of the desired product was formed, respectively (Figure 5). We also observed moderate and high levels of conversion for the benzotriazole fragment **8** in the high-throughput screen in reaction A and B, respectively. As predicted by these results, substrate **24** afforded the desired product in 49% (13:87 *b:l*) and 75% (10:90 *b:l*) yield (reaction A and B, respectively). The lack of regiodivergence observed for **24** in both reaction conditions is unusual and there may be a substrate-specific steric or electronic basis for this observed regiochemical outcome. Interestingly, addition of fragment **8** does not result in reversal of regiocontrol in the formation of **2** in reaction A (78:22 *b:l*) (Figure 4). Similarly, addition of fragment **5** does not attenuate regiocontrol of **2** in reaction A (77:23 *b:l*). As anticipated, piperidine-, imidazole-, and pyridine-containing scaffolds (**25**, **26**, and **27**) were poor substrates in both reactions. It has yet to be determined how broadly

applicable such an analysis would be for other classes of chemical transformations in which steric and electronic considerations may play an important role.

Blocking strategies for Lewis basic heterocycles

As previously alluded to, the pyridine functionality has been demonstrated to be an especially effective directing group in chelation-mediated Pd-catalyzed C–H activation methodology.[8,41,42] As such, we correctly anticipated that the influence of this functionality, typical of the effects exerted by some of the more strongly Lewis basic moieties, would be among the more difficult to circumvent in non-directed C–H activation protocols.[41] The high-throughput screen with pyridine as an additive (Figure 4), as well as a reaction screen employing a pyridine-containing substrate (entries 1 and 2, Table 1), arrested catalyst activity in both of the allylic C–H functionalization methods attempted.

However, pyridine is a structural motif prevalent in pharmaceutically-relevant compounds, and consequently there exists a need for developing blocking strategies to enable its use in C–H functionalization synthetic methods. Therefore, pyridine was selected as an ideal model for evaluation of blocking strategies. As previously mentioned, no desired allylic C–H acetoxylation product was observed when a pyridine moiety was present within the substrate (entries 1 and 2, Table 1). However, as exemplified in Figure 2, when this pendant Lewis basic nitrogen-containing functionality was replaced with a simple phenyl ring, both allylic C–H functionalization reaction conditions furnished the desired allylic acetoxylation product with high levels of regioselectivity for either the branched (**29**) or linear (**30**) allylic acetate regioisomer (entries 3 and 4). Interestingly, the terminal oxidant employed using a $Pd(OAc)_2$/4,5-diazafluorenone-catalyst system could be changed to O_2 from *p*-benzoquinone with comparable yield without loss of regiocontrol (entry 4 vs. 5). The ability to interchange terminal oxidants has potential mechanistic implications that will be addressed in due course. Additionally, employing *p*-benzoquinone in place of O_2 is more practical from a technical standpoint in parallel synthesis efforts.

We hoped to block pyridine coordination of the Pd(II)-catalyst by adding a sacrificial Lewis or Brønsted acid and thereby circumvent catalyst arrest. In an automated screen of Lewis and Brønsted acids, it was discovered that only $Sc(OTf)_3$ and BF_3•OEt_2 among a long list were moderately effective as *in situ* pyridine-blocking groups (entries **6–8**). BF_3•OEt_2 was identified as the most effective *in situ* blocking reagent so far, allowing 38% isolated yield of desired product. In comparison, the “control” substrate (lacking the pyridine nitrogen) for this reaction afforded product in comparable 51% isolated yield (entry 3), albeit with higher regioselectivity. The lower regiocontrol observed in these reactions employing Lewis acid additives is postulated to result from a Lewis acid-assisted Pd-catalyzed allylic transposition rather than from a change in reaction mechanism.[43] Additionally, the use of Lewis acid additives presumably affects reduced catalyst turnover, evident from the lower overall yield of desired product. No product formation was observed under reaction conditions B or C using the $Pd(OAc)_2$/4,5-diazafluorenone-catalyst system when $Sc(OTf)_3$ or BF_3•OEt_2 were added (entries **9–11**).

Pre-forming a pyridine *N*-oxide proved to be a far more effective and generally applicable covalent blocking strategy, permitting both sets of reaction conditions employed to furnish

the desired product in good yields (entries 12 and 13, Table 1). Alternate covalent blocking strategies such as pyridinium *N*-acyl, *N*-silyl, or *N*-alkyl may ultimately prove similarly useful in this or related systems.

Computational studies of binding affinities of heterocycles to Pd(II)L_n

Within the set of heterocycles screened in Figure 4, there may be three major pathways associated with catalyst arrest: (***i***) a 1:1 coordination of heterocycle:Pd(II)L_n, (***ii***) a 2:1 coordination of heterocycle:Pd(II)L_n, or alternatively, (***iii***) sp^2 C–H insertion of a heterocycle by the Pd(II)L_n catalyst.[44–49] Empirically, it is observed that heterocycles with higher expected Lewis basicities lead to lower overall product conversion in both C–H oxidation methods, which may be related to coordination-related reduction of reaction rates. Efforts are currently underway to elucidate the heterocycle–Pd(II) speciation as well as to study rates of reaction.

Eager to understand the theoretical basis for the trends observed in our high-throughput heterocycle screen (Figure 4), we hypothesized that the discrete binding affinities of the Lewis basic fragments to the Pd(II)L_n catalysts may have inverse correlations with the levels of product conversion observed in both reaction screens. It should be noted that there are limited data in the literature evaluating the binding affinity of heterocycles to transition metal catalysts, with most reports focused rather on the binding affinity of ligands (such as phosphines, *N*-heterocyclic carbenes, etc.) to transition metals.[50–55] To the best of our knowledge, a study linking the experimental efficacy of an active transition metal catalyst to its putative coordination-mediated arrest has not been previously described.

We calculated the binding affinity of the heterocycles illustrated in Figure 4 to a $Pd(OAc)_2$-system using density functional theory (DFT). DFT methods, such as M06, that better account for dispersion interactions have been shown to give relatively accurate metal–ligand bond energies.[54,55] The $Pd(OAc)_2$ catalyst system served as a simple model, providing theoretical heterocycle–$Pd(OAc)_2$ binding affinities without the influence of either the $PhS(O)C_2H_4S(O)Ph$ or the 4,5-diazafluorenone ligand. Coordination of Pd with either of these ligands will influence the binding affinity of a heterocyclic Lewis base to the Pd(II)L_n species to varying magnitudes. It was calculated that the $Pd(OAc)_2$/$PhS(O)C_2H_4S(O)Ph$ complex is endergonic by 1.9 kcal/mol with respect to an unbound $Pd(OAc)_2$-species, which is the putative resting state of the catalyst. The predominance of unbound $Pd(OAc)_2$ in the presence of $PhS(O)C_2H_4S(O)Ph$ has also been observed experimentally.[56,57] In contrast, the $Pd(OAc)_2$/4,5-diazafluorenone complex is exergonic by 4.2 kcal/mol with respect to unbound $Pd(OAc)_2$, indicating that the latter is not the resting state in this catalytic system (see the Supplementary Information for details). We also considered the involvement of a Lewis base-coordinated Pd-π-allyl species in these studies of theoretical binding affinities (see the Supplementary Information for further details).

Based on the above analysis, for reaction A, $Pd(OAc)_2$ served as an ideal candidate for studying theoretical binding affinities to the heterocycles illustrated in Figure 4. A reasonable correlation is observed between the theoretical heterocycle–$Pd(OAc)_2$ binding affinities and product conversion for reaction A (**a**, Figure 6). The binding affinity of propene to $Pd(OAc)_2$ was also computed as a model for the terminal alkene substrate (red

line in Figure 6); the majority of heterocycles that inhibit reactivity in reaction A have theoretical binding affinities greater than that of propene. A poorer correlation is observed between the theoretical heterocycle–$Pd(OAc)_2$ binding affinities and product conversion for reaction B (**b**). Catalyst inactivation is clearly more complex in the presence of the 4,5-diazafluorenone ligand, possibly due to steric effects and multiple coordination modes (see the Supplementary Information for more details). However, a full examination of heterocycle-binding to the relevant catalytic intermediates will require a thorough exploration of the reaction mechanism, which is planned for future studies. When a 2:1 coordination of heterocycle–$Pd(OAc)_2$ is computed, the correlation observed between the theoretical binding affinities and product conversion is slightly improved for reaction A (**c**). However, 2:1 heterocycle–$Pd(OAc)_2$ interactions do not significantly alter the poor correlation observed for reaction B (**d**). As indicated previously, while many heterocycles may be coordinating with the Pd and detrimentally effecting reaction outcome, there may be other pathways leading to catalyst arrest. As a general trend, however, the heterocycles with lower relative theoretical binding affinities with respect to a propene moiety allowed for the highest product conversions observed.

As our understanding of the active Pd(II)-catalyst species as well as the exact nature of catalyst arrest expands, *de novo* design of a heterocycle-containing substrate may be possible where a structure is computationally conceived to have a lower theoretical binding affinity than the desired olefin functionality. Such analysis could provide a theoretical model to estimate the ability of the transition metal catalyst to perform efficaciously in the presence of a desired Lewis basic moiety. Additionally, as we further understand the fundamental nature of the active catalyst, these results could help inform next generation ligand synthesis, where ligands may be designed so that the theoretical heterocycle–ML_n binding affinities are minimized. This could result in the synthesis of a ML_n species that may be more robust to the presence of Lewis basic heteroaromatics. Efforts to realize these concepts are ongoing and will be reported in due course. Overall, the theoretical investigation of these systems has implications not only in the class of reactions studied herein, but in a wide array of transition metal-catalyzed transformations where there may be similar ML_n–Lewis base interactions.

NMR binding studies of heterocycles to $Pd(OAc)_2$

In order to bridge the understanding between the theoretical binding affinities and the experimental results, we measured the binding of the heterocycles illustrated in Figure 4 to $Pd(OAc)_2$ by ^1H NMR analysis (binding data for each ligand is included in the Supplementary Information). Binding to Pd was quantitated by the disappearance of the parent ligand with 1:1 ligand:$Pd(OAc)_2$. Interestingly, the majority of ligands displayed either complete binding to Pd, or none at all, with only a handful exhibiting intermediate binding. There is a clear trend that ligands which tightly bind Pd (as evidenced by ^1H NMR analysis) also allow little to no reaction conversion in the high-throughput ligand screen for reaction A (**a**, Figure 7). Conversely, the less tightly bound ligands enable reaction conversion. These experimental ^1H NMR data aid in corroborating the trends observed in the theoretical binding studies in reaction A (**a** and **c**, Figure 6). When comparing the ^1H NMR binding of the heterocycles to the experimental results from reaction B (**b**, Figure 7), a trend for the less tightly bound ligands enabling a higher degree of reaction conversion is

also observed. However, multiple ligands that display 100% Pd-binding permit reasonable reaction conversions in the high-throughput screen, which may be due to kinetic parameters governing exchange of these ligands and olefin substrate when bound to Pd. These data help corroborate the observed trends in the theoretical binding studies for reaction B (**b** and **d**, Figure 6), mimicking the higher degree of scatter, presumably resulting from a more complex experimental system.

Conclusions

We have demonstrated that Lewis basic sites within reaction substrates cause the attenuation of catalyst activity in Pd(II)-catalyzed allylic C–H functionalization methods. A high-throughput robustness screen was utilized to rapidly estimate the impact of heterocycles on catalyst performance under the selected reaction conditions. We performed a broad Lewis and Brønsted acid screen, from which it was determined that BF_3•OEt_2 enabled desired C–H oxidation, which we propose is due to *in situ* blocking of the pyridine basic nitrogen. An alternate and higher yielding strategy was realized through covalent blocking of the Lewis basic site. Pre-forming the corresponding pyridine *N*-oxide prior to the C–H functionalization step afforded the desired oxidation product in synthetically useful yields. Theoretical studies were undertaken to determine the binding affinities of selected heterocycles to a simple $Pd(OAc)_2$ model system. An inverse correlation was observed between the binding affinity to the level of product conversion. Corroborating ^{1}H NMR binding studies between ligand and $Pd(OAc)_2$ were also performed, showing a trend between a high-throughput ligand screen, theoretical binding studies, and ^{1}H NMR binding studies. These combined results are expected to have implications not limited to the methods demonstrated herein, but to a variety of chemical synthesis protocols that suffer from deleterious effects when attempted on substrates containing Lewis basic moieties. Additional studies are underway to explore the mechanistic and theoretical implications of our present results, to further optimize *in situ* blocking strategies, and to explore other transformations that could benefit from similar analyses.

Supplementary Material

Refer to Web version on PubMed Central for supplementary material.

Acknowledgments

The authors thank Professor M. Christina White for helpful discussions. The authors thank Professor Matthew S. Sigman for helpful discussions and suggestions. H.A.M. thanks Dr. Audrey G. Ross, Dr. Jing He, and Dr. Rohan Beckwith for helpful discussions and suggestions. H.A.M. gratefully acknowledges the Education Office of the Novartis Institutes for BioMedical Research, Inc. for receipt of a Presidential Postdoctoral Research Fellowship. B.L.H.T. gratefully acknowledges the National Institute of Health for a postdoctoral fellowship (F32GM106596). B.L.H.T., K.N.H., and J.D.B. gratefully acknowledge the National Science Foundation under the CCI Center for Selective C–H Functionalization (Grant CHE-1205646). Computational resources were provided by the UCLA Institute for Digital Research and Education (IDRE) and the Extreme Science and Engineering Discovery Environment (XSEDE), which is supported by the NSF.

Notes and references

1. Crabtree RH. Chem Rev. 1985; 85:245–269.
2. Shilov AE, Shul’pin GB. Chem Rev. 1997; 97:2879–2932. [PubMed: 11851481]

3. Ritleng V, Sirlin C, Pfeffer M. Chem Rev. 2002; 102:1731–1770. [PubMed: 11996548]
4. Labinger JA, Bercaw JE. Nature. 2002; 417:507–514. [PubMed: 12037558]
5. Yu JQ, Giri R, Chen X. Org Biomol Chem. 2006; 4:4041–4047. [PubMed: 17312954]
6. Bergman RG. Nature. 2007; 446:391–393. [PubMed: 17377575]
7. Hartwig JF. Nature. 2008; 455:314–322. [PubMed: 18800130]
8. Lyons TW, Sanford MS. Chem Rev. 2010; 110:1147–1169. [PubMed: 20078038]
9. Engle KM, Mei TS, Wasa M, Yu JQ. Acc Chem Res. 2011; 45:788–802. [PubMed: 22166158]
10. Brückl T, Baxter RD, Ishihara Y, Baran PS. Acc Chem Res. 2011; 45:826–839. [PubMed: 22017496]
11. Neufeldt SR, Sanford MS. Acc Chem Res. 2012; 45:936–946. [PubMed: 22554114]
12. Yamaguchi J, Yamaguchi AD, Itami K. Angew Chem Int Ed. 2012; 51:8960–9009.
13. Wencel-Delord J, Glorius F. Nat Chem. 2013; 5:369–375. [PubMed: 23609086]
14. Popp, B.; Stahl, S. Organometallic Oxidation Catalysis. Meyer, F.; Limberg, C., editors. Vol. 22. Springer; Berlin Heidelberg: 2007. p. 149-189.ch. 39
15. Liu, G.; Wu, Y. C–H Activation. Yu, J-Q.; Shi, Z., editors. Vol. 292. Springer; Berlin Heidelberg: 2010. p. 195-209.ch. 16
16. Campbell AN, Stahl SS. Acc Chem Res. 2012; 45:851–863. [PubMed: 22263575]
17. Chen MS, White MC. J Am Chem Soc. 2004; 126:1346–1347. [PubMed: 14759185]
18. Chen MS, Prabagaran N, Labenz NA, White MC. J Am Chem Soc. 2005; 127:6970–6971. [PubMed: 15884938]
19. Fraunhoffer KJ, Prabagaran N, Sirois LE, White MC. J Am Chem Soc. 2006; 128:9032–9033. [PubMed: 16834366]
20. Delcamp JH, White MC. J Am Chem Soc. 2006; 128:15076–15077. [PubMed: 17117844]
21. Stang EM, White MC. Nat Chem. 2009; 1:547–551. [PubMed: 21378935]
22. Vermeulen NA, Delcamp JH, White MC. J Am Chem Soc. 2010; 132:11323–11328. [PubMed: 20662536]
23. Campbell AN, White PB, Guzei IA, Stahl SS. J Am Chem Soc. 2010; 132:15116–15119. [PubMed: 20929224]
24. Hoveyda AH, Evans DA, Fu GC. Chem Rev. 1993; 93:1307–1370.
25. Roughley SD, Jordan AM. J Med Chem. 2011; 54:3451–3479. [PubMed: 21504168]
26. Walters WP, Green J, Weiss JR, Murcko MA. J Med Chem. 2011; 54:6405–6416. [PubMed: 21755928]
27. Nadin A, Hattotuwagama C, Churcher I. Angew Chem Int Ed. 2012; 51:1114–1122.
28. Churcher I. Nat Chem. 2013; 5:554–555. [PubMed: 23787741]
29. Campeau LC, Rousseaux S, Fagnou K. J Am Chem Soc. 2005; 127:18020–18021. [PubMed: 16366550]
30. Leclerc JP, Fagnou K. Angew Chem Int Ed. 2006; 45:7781–7786.
31. Kanyiva KS, Nakao Y, Hiyama T. Angew Chem Int Ed. 2007; 46:8872–8874.
32. Nakao Y, Kanyiva KS, Hiyama T. J Am Chem Soc. 2008; 130:2448–2449. [PubMed: 18247621]
33. Nakao Y, Yamada Y, Kashihara N, Hiyama T. J Am Chem Soc. 2010; 132:13666–13668. [PubMed: 20822182]
34. Shen Q, Hartwig JF. J Am Chem Soc. 2007; 129:7734–7735. [PubMed: 17542591]
35. Kuhl N, Hopkinson MN, Wencel-Delord J, Glorius F. Angew Chem Int Ed. 2012; 51:10236–10254.
36. Duez S, Steib AK, Manolikakes SM, Knochel P. Angew Chem Int Ed. 2011; 50:7686–7690.
37. Huang J, Haar CM, Nolan SP, Marcone JE, Moloy KG. Organometallics. 1999; 18:297–299.
38. van Otterlo WAL, de Koning CB. Chem Rev. 2009; 109:3743–3782. [PubMed: 19618929]
39. (a) Collins KD, Glorius F. Nat Chem. 2013; 5:597–601. [PubMed: 23787750] (b) Collins KD, Glorius F. Tetrahedron. 2013; 69:7817–7825.(c) Rühling A, Lied F, Glorius F. Chem Eur J. in addition, a high-throughput robustness screen was an integral part of the following studies. 10.1002/chem.201304508(d) Tang D-TD, Collins KD, Ernst JB, Glorius F. Angew Chem Int Ed.

10.1002/anie.201309305(e) Kuhl N, Schröder N, Glorius F. Org Lett. 2013; 15:3860–3863. [PubMed: 23906080]

40. Düfert MA, Billingsley KL, Buchwald SL. J Am Chem Soc. 2013
41. Dick AR, Hull KL, Sanford MS. J Am Chem Soc. 2004; 126:2300–2301. [PubMed: 14982422]
42. Chen X, Goodhue CE, Yu JQ. J Am Chem Soc. 2006; 128:12634–12635. [PubMed: 17002342]
43. Overman LE, Knoll FM. Tetrahedron Lett. 1979; 20:321–324.
44. Steinhoff BA, Guzei IA, Stahl SS. J Am Chem Soc. 2004; 126:11268–11278. [PubMed: 15355108]
45. Schultz MJ, Adler RS, Zierkiewicz W, Privalov T, Sigman MS. J Am Chem Soc. 2005; 127:8499–8507. [PubMed: 15941285]
46. Zhang YH, Shi BF, Yu JQ. J Am Chem Soc. 2009; 131:5072–5074. [PubMed: 19296661]
47. Emmert MH, Cook AK, Xie YJ, Sanford MS. Angew Chem Int Ed. 2011; 50:9409–9412.
48. Zhang S, Shi L, Ding Y. J Am Chem Soc. 2011; 133:20218–20229. [PubMed: 22112165]
49. Kubota A, Emmert MH, Sanford MS. Org Lett. 2012; 14:1760–1763. [PubMed: 22409653]
50. Cedeno DL, Weitz E. J Am Chem Soc. 2001; 123:12857–12865. [PubMed: 11749544]
51. Frenking G, Wichmann K, Frohlich N, Grobe J, Golla W, Le Van D, Krebs B, Lage M. Organometallics. 2002; 21:2921–2930.
52. Diedrich C, Luchow A, Grimme S. J Chem Phys. 2005:122.
53. Zhao Y, Truhlar DG. Org Lett. 2007; 9:1967–1970. [PubMed: 17428063]
54. Fey N, Ridgway BM, Jover J, McMullin CL, Harvey JN. Dalton Trans. 2011; 40:11184–11191. [PubMed: 21853190]
55. Chen M, Craciun R, Hoffman N, Dixon DA. Inorg Chem. 2012; 51:13195–13203. [PubMed: 23194426]
56. Diao T, White P, Guzei I, Stahl SS. Inorg Chem. 2012; 51:11898–11909. [PubMed: 23092381]
57. Young AJ, White MC. Angew Chem Int Ed. 2011; 50:6824–6827.

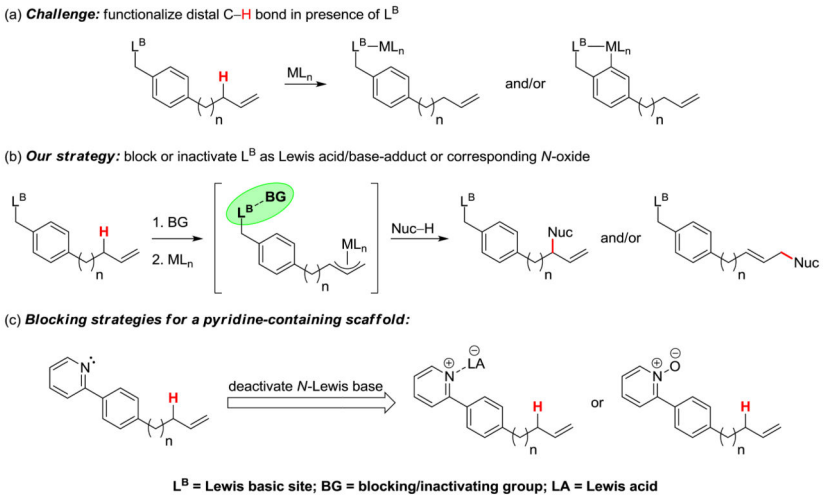

Figure 1.

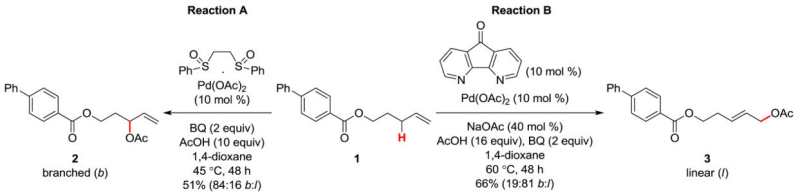

Figure 2.

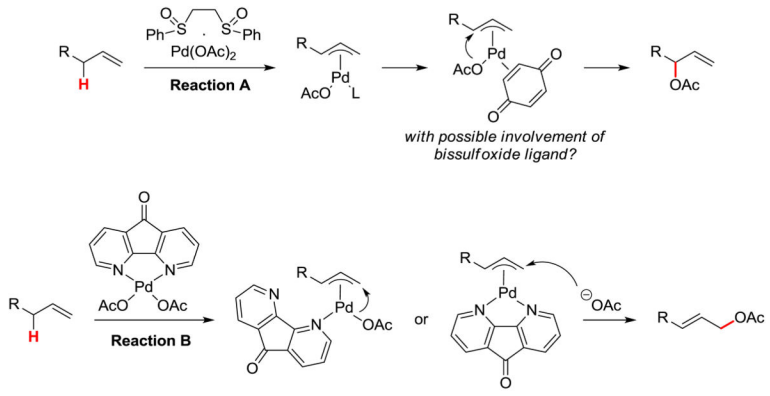

Figure 3.

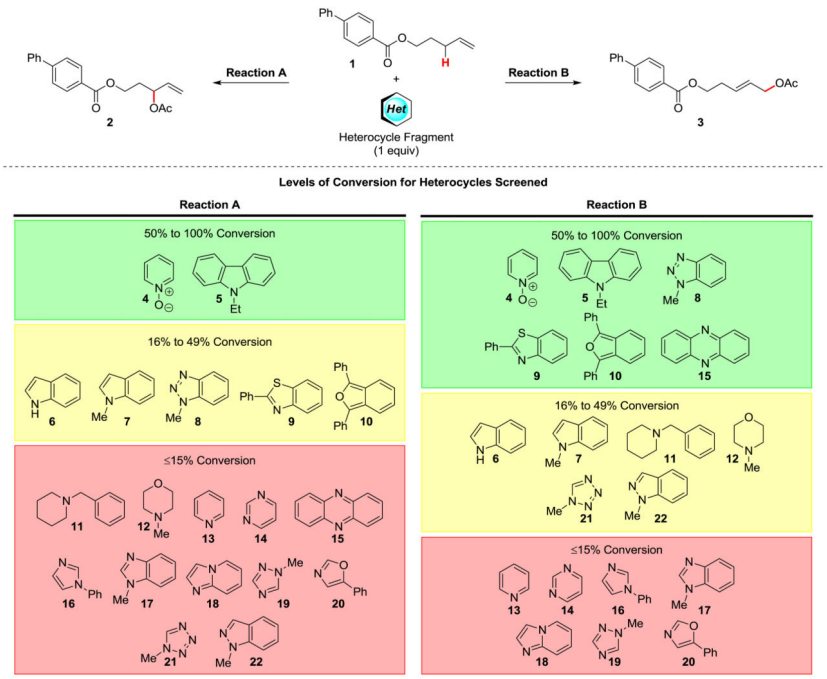

Figure 4.

Reaction conditions **A**: $Pd(OAc)_2$/$PhS(O)C_2H_4S(O)Ph$ (10 mol %), *p*-benzoquinone (2 equiv), AcOH (10 equiv), 1,4-dioxane (0.3 M), 45 °C, 48 h; **B**: $Pd(OAc)_2$ (10 mol %), 4,5-diazafluorenone (10 mol %), *p*-benzoquinone (2 equiv), NaOAc (40 mol %), AcOH (16 equiv), 1,4-dioxane (0.3 M), 60 °C, 48 h. Compiled results of the high-throughput heterocycle screen. Heterocycles are separated into three tiers for both reaction A and B; the colors represent the following for each reaction: **green** (50% to 100% product conversion), **yellow** (16% to 49% conversion), and **red** (≤15% product conversion). Conversion is defined as % product formation by HPLC relative to remaining starting material.

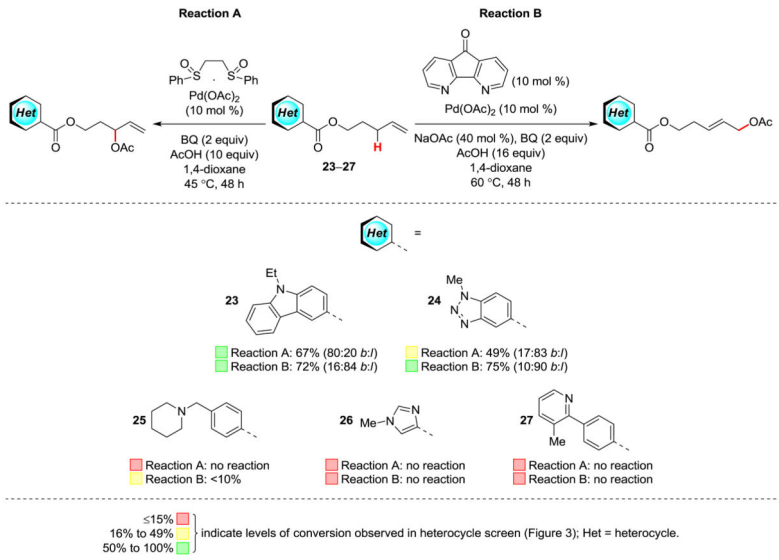

Figure 5.

Validation of the potential predictive qualities of the high-throughput heterocycle screen employed (see Figure 4). Five representative heterocycles from the high-throughput screen were incorporated within substrates that were subjected to Pd(II)-catalyzed allylic C–H acetoxylation. Reaction conditions **A**: $Pd(OAc)_2$/$PhS(O)C_2H_4S(O)Ph$ (10 mol %), *p*-benzoquinone (2 equiv), AcOH (10 equiv), 1,4-dioxane (0.3 M), 45 °C, 48 h; **B**: $Pd(OAc)_2$ (10 mol %), 4,5-diazafluorenone (10 mol %), *p*-benzoquinone (2 equiv), NaOAc (40 mol %), AcOH (16 equiv), 1,4-dioxane (0.3 M), 60 °C, 48 h. Isolated yields reported.

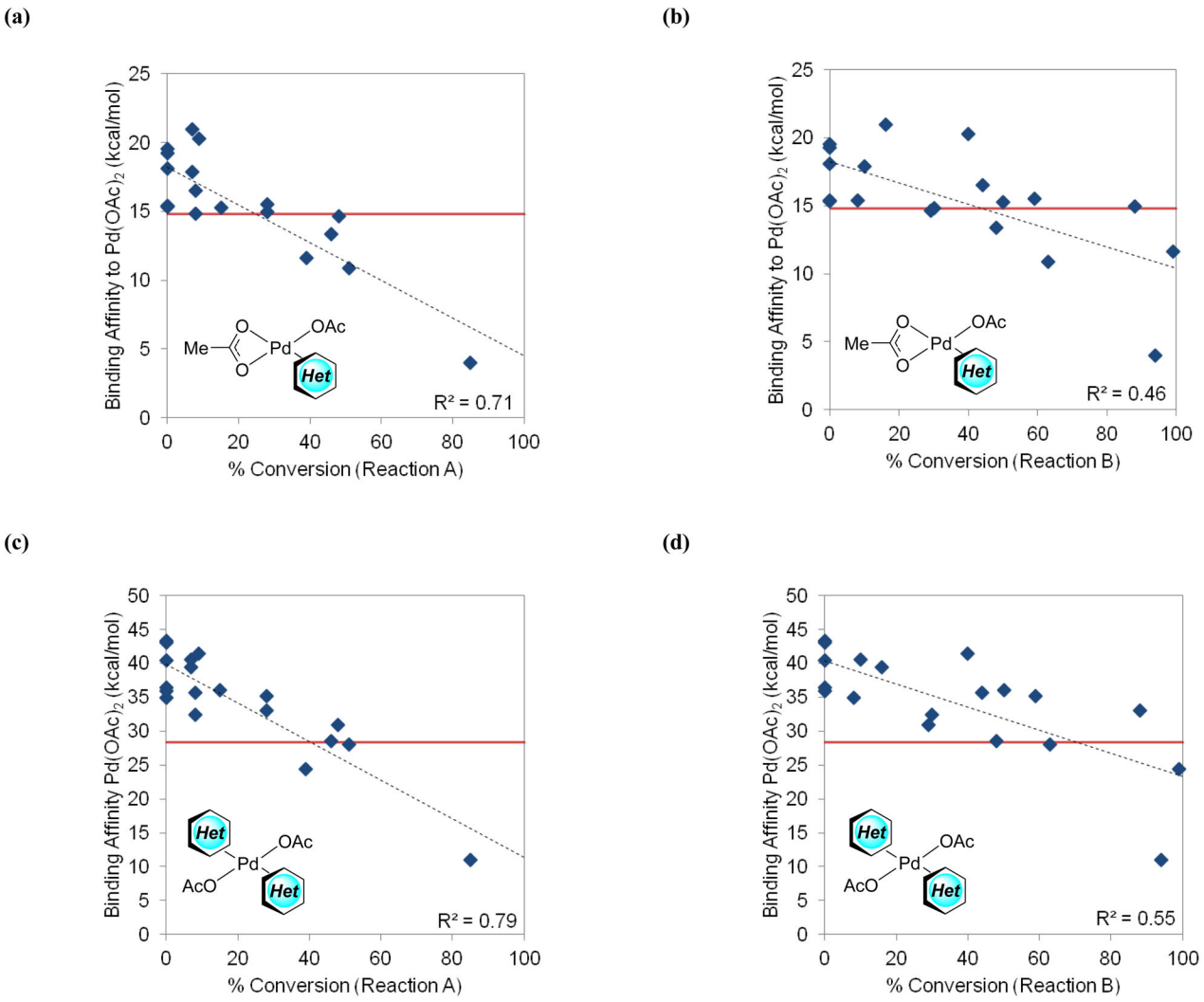

Figure 6.

Theoretical binding affinities of heterocycles to $Pd(OAc)_2$ vs. product conversion (%) observed in reaction A (**a**) and reaction B (**b**); Theoretical binding affinities of heterocycles to $Pd(OAc)_2$ to form a 2:1 complex vs. product conversion (%) observed in reaction A (**c**) and reaction B (**d**). Binding affinity is defined as $-\Delta H$ for the reaction L + $Pd(OAc)_2 \rightarrow LPd(OAc)_2$ (**a** and **b**) or 2 L + $Pd(OAc)_2 \rightarrow L_2Pd(OAc)_2$ (**c** and **d**). The horizontal red line indicates the binding affinity of propene. Geometries were optimized at the B3LYP/SDD–6–31G(d,p) level with single-point energies computed at the M06/SDD(f)–6–311++G(2d,p) level with SMD solvation model (1,4-dioxane); see the Supplementary Information for data with acetic acid. Product conversions and corresponding reaction conditions A and B are based on the high-throughput heterocycle screen (Figure 4). Each data point represents a specific heterocycle fragment from Figure 4.

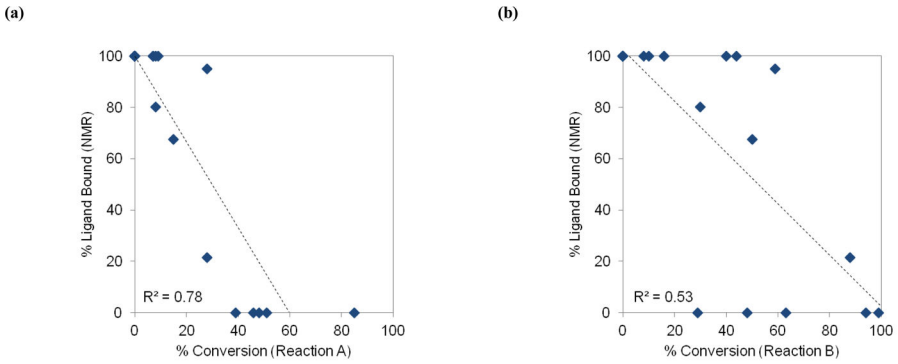

Figure 7.

^{1}H NMR binding values of heterocycles to $Pd(OAc)_2$ vs. product conversion (%) observed in reaction A (**a**) and reaction B (**b**). Binding values were determined by quantitating disappearance of parent ligand by ^{1}H NMR with 1:1 ligand/$Pd(OAc)_2$. Product conversions and corresponding reaction conditions A and B are based on the high-throughput heterocycle screen (Figure 4). Each data point represents a specific heterocycle fragment from Figure 4.

Table 1

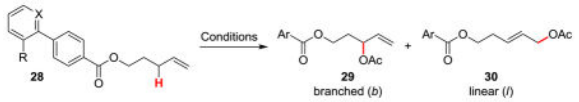

	Entry	X	R	Conditions [a]	Additive	% Yield	Regiosel. (29:30) [b]
Control Reactions	1	N	Me	A	---	0	---
	2	N	Me	B	---	0	---
	3	CH	H	A	---	51	84:16
	4	CH	H	B	---	66	19:81
	5	CH	H	C	---	58	18:82
Lewis Acid Additives	6	N	Me	A	$Sc(OTf)_3$ (1 equiv)	8	27:73
	7	N	Me	A	$BF_3{\bullet}OEt_2$ (1 equiv)	21	32:68
	8	N	Me	A	$BF_3{\bullet}OEt_2$ (2 equiv)	38	30:70
	9	N	Me	B or C	$Sc(OTf)_3$ (1 equiv)	0	---
	10	N	Me	B or C	$BF_3{\bullet}OEt_2$ (1 equiv)	0	---
	11	N	Me	B or C	$BF_3{\bullet}OEt_2$ (2 equiv)	0	---
N-Oxides	12	NO	Me	A [c]	---	61	88:12
	13	NO	Me	C	---	77	9:91

[a] Conditions: **A**: $Pd(OAc)_2$/$PhS(O)C_2H_4S(O)Ph$ (10 mol %), *p*-benzoquinone (2 equiv), AcOH (10 equiv), 1,4-dioxane (0.3 M), 45 °C, 48 h; **B**: $Pd(OAc)_2$ (10 mol %), 4,5-diazafluorenone (10 mol %), *p*-benzoquinone (2 equiv), NaOAc (40 mol %), AcOH (16 equiv), 1,4-dioxane (0.3 M), 60 °C, 48 h. **C**: $Pd(OAc)_2$ (10 mol %), 4,5-diazafluorenone (10 mol %), O_2 (1 atm), NaOAc (40 mol %), AcOH (16 equiv), 1,4-dioxane (0.3 M), 60 °C, 48 h.

[b] Ratios determined by crude ^1H NMR analysis.

[c] $MeOC_6H_4CO_2H$ (5 equiv) used in place of AcOH.